

Imaging of spinor gases

Iacopo Carusotto^{1,2} and Erich J. Mueller³¹Laboratoire Kastler Brossel, Ecole Normale Supérieure,
24 rue Lhomond, 75231 Paris Cedex 05, France²BEC-INFM Research and Development Center, I-38050 Povo, Trento, Italy³Laboratory of Atomic and Solid State Physics, Cornell University, Ithaca, New York 14853
(Dated: February 7, 2020)

We explain how polarized light can be used to image spin textures in cold atomic gases. This technique directly probes the underlying geometric properties of the order parameter.

PACS numbers: 03.75.Mn, 42.30.-d, 03.75.Lm

Superfluids display dramatic rotational properties. For example, arrays of quantized vortices have been observed in rotating gaseous spin-polarized ^{87}Rb and ^{23}Na Bose-Einstein condensates (BECs) [1]. The physics of rotating systems is even richer in the presence of spin degrees of freedom: thanks to the interplay of the spin and translational degrees of freedom, simple vortices are replaced by more complicated spin textures. These textures have been studied in many different contexts, from $^3\text{He-A}$ [2] to quantum Hall systems [3] and, more recently, trapped gaseous BECs [4, 5, 6, 7].

Theoretical studies have analyzed the structure of spin textures in rotating spinor BECs for different values of the spin, the trap rotation frequency, and the atom-atom interactions [4, 5]. Experimental studies, beginning with pseudo-spin-1=2 systems [6] and continuing with spin-1 and spin-2 condensates [7], have observed individual spin textures. These experiments are complemented by studies of spin dynamics in non-rotating spin-1 and spin-2 clouds [8].

In most of these experiments [9], imaging is performed by first separating the different spin components using a magnetic field gradient (the method pioneered by Stern and Gerlach [10]). The spin components are then separately imaged via conventional optical absorption or phase contrast techniques. This approach is intrinsically destructive and is unable to probe coherences between the different spin components. Moreover, images of the individual components are very sensitive to global rotations of the order parameter [5].

In the present paper, we propose a different imaging scheme which should be able to provide non-destructive, in-situ, images of the spin textures and which directly addresses the geometric properties of the BEC order parameter. The method relies on the dependence of the dielectric properties of a spinor atomic gas on the internal state of the atoms. Focussing our attention on the case of spin-1 atoms, we derive a simple expression of the local dielectric tensor $\epsilon_{ij}(\mathbf{x})$ in terms of the local density $n(\mathbf{x})$, spin density $\mathbf{S}(\mathbf{x})$, and nematic order parameter $N_{ij}(\mathbf{x})$ of the atomic gas. Using this expression for $\epsilon_{ij}(\mathbf{x})$, we then study the propagation of polarized light across an atomic

cloud: we show how information about the spatial profile of the spin texture can be retrieved by analyzing the intensity, phase, and polarization profile of the transmitted light. Our technique has analogies in other areas of condensed matter physics: the polarization of the electrons in a solid-state sample [11] as well as the order parameter of nematic liquid crystals [12] can be measured by looking at polarization changes in a transmitted, directed, or reflected light. Because of its complex nature, the order parameter of spin-1 atomic systems can have both a vectorial (spin) and a tensorial (nematic) components at the same time: possible ways of separating the contribution of each of them are here discussed.

The electric-dipole Hamiltonian describing the interaction of light with a two-level atom can be written in a second-quantized form as:

$$H_{\text{int}} = \sum_i \int d\mathbf{x} \sum_{\alpha, \beta} D_{i\alpha}^\dagger \hat{E}_i^\alpha(\mathbf{x}) \hat{E}_i^\beta(\mathbf{x}) \hat{c}_{i\beta} \quad (1)$$

The atomic field operators $\hat{c}_i^\alpha(\mathbf{x})$ and $\hat{c}_i^\beta(\mathbf{x})$ destroy an atom at spatial position \mathbf{x} in respectively the sublevel of the excited state or the sublevel of the ground state. $\hat{E}_i^\alpha(\mathbf{x})$ is the i -component of the electric field operator at \mathbf{x} and $D_{i\alpha} = \langle \alpha | \hat{d}_i | \beta \rangle$: i gives the matrix element of the i -component of the electric dipole moment between the sublevels α and β of respectively the excited and ground state.

For light frequencies ω well detuned from the resonance frequency ω_0 of the $g \rightarrow e$ transition, we can eliminate the excited state and write an effective Hamiltonian for the ground state atoms coupled to the electromagnetic field:

$$H_{\text{int}} = \sum_{ij} \int d\mathbf{x} \sum_{\alpha, \beta} U_{ij\alpha\beta} \hat{E}_i^\alpha(\mathbf{x}) \hat{E}_j^\beta(\mathbf{x}) \hat{c}_i^\alpha \hat{c}_j^\beta \quad (2)$$

where the U tensor is defined as:

$$U_{ij\alpha\beta} = \frac{1}{\omega - \omega_0} \sum_{\gamma, \delta} D_{i\gamma} D_{j\delta} \quad (3)$$

In our case of spin-1 atoms, the matter field is vectorial and can be described by its cartesian components

$(\hat{x}; \hat{y}; \hat{z})$ [13]. The local one-body density-matrix $m_{ij}(\mathbf{x}) = \hat{y}_i(\mathbf{x}) \hat{z}_j(\mathbf{x})$ can therefore be decomposed into its three tensorial components of angular momentum respectively 0, 1 and 2, whose explicit expressions in cartesian components are:

$$\rho(\mathbf{x}) = \sum_j m_{jj}(\mathbf{x}) = \hat{y}(\mathbf{x}) \hat{z}(\mathbf{x}) \quad (4)$$

$$S_j(\mathbf{x}) = \frac{1}{i} \epsilon_{jkl} m_{kl}(\mathbf{x}) = \frac{1}{i} \hat{y}(\mathbf{x}) \hat{z}(\mathbf{x}) \quad (5)$$

$$N_{ij}(\mathbf{x}) = \frac{1}{2} [m_{ij}(\mathbf{x}) + m_{ji}(\mathbf{x})] - \frac{\delta_{ij}}{3} \rho(\mathbf{x}) \quad (6)$$

The totally antisymmetric unit tensor is denoted ϵ_{jkl} . Physically, the scalar ρ corresponds to the total density, the vector S to the spin density, and the second-rank, symmetric tensor N to the nematicity (or quadrupole moment). An identical decomposition into the intensity I , the spin density S and the nematicity N can be performed for the electromagnetic field one-body density matrix defined as $f_{ij} = \hat{E}_i^y \hat{E}_j^z$.

As scalars can only be formed by contracting quantities of same angular momentum, the Hamiltonian (2) can be parametrized in terms of just three real quantities $b_{0;1;2}$:

$$H_{\text{int}} = \int d\mathbf{x} \left[b_0 I(\mathbf{x}) + b_1 S(\mathbf{x}) + b_2 \sum_{ij} N_{ij}(\mathbf{x}) N_{ij}(\mathbf{x}) \right] \quad (7)$$

This form of the light-matter Hamiltonian can be useful for studying the optical potential induced by light on atoms, as well as the refractive index observed by light while crossing the atomic sample.

In the first case, a scalar potential comes from the local intensity $I(\mathbf{x})$ of light, a pseudo-magnetic field comes from the electromagnetic spin $S(\mathbf{x})$, and the $N(\mathbf{x})$ tensor couples to the nematicity $N(\mathbf{x})$ of the atoms. A first application of this formalism has been given in [16], where effects arising from a kind of spin-orbit coupling induced by the pseudo-magnetic field is analyzed in detail for atoms propagating in suitably designed optical lattices.

In the present paper, we concentrate on the second class of phenomena, namely on how the optical properties of the atomic cloud depend on the spin state of the atoms; in particular we shall discuss how the polarization state of a light beam after crossing the atomic sample can be used to obtain information on the spin state of the atoms.

Under a mean-field approximation in which the quantum correlations between the matter and the light field are neglected, a wave equation for the eigenmodes of the electromagnetic field in a homogeneous medium can be directly obtained from the Hamiltonian (2):

$$-\nabla^2 \mathbf{E} = c^2 \mathbf{P} \mathbf{E} \quad (8)$$

where the projector \mathbf{P} projects orthogonally to the wavevector \mathbf{k} and the tensor \mathbf{P} has been defined as:

$$P_{jk} = U_{ijk1} m_{il} \quad (9)$$

By comparing this wave equation with the Fresnel equation for a generic medium of dielectric tensor ϵ :

$$\left(\frac{\omega^2}{c^2} - \epsilon \right) \mathbf{E} = 0 \quad (10)$$

one obtains the following explicit expression for the dielectric constant of our atomic sample at the frequency ω in terms of the coupling tensor U in the cartesian basis and the one-body density matrix m :

$$\epsilon_{jk} = \epsilon_0 \delta_{jk} + \frac{2}{\omega^2} U_{ijk1} m_{il} \quad (11)$$

The same symmetry arguments previously used to parametrize the Hamiltonian in the form (7) lead to the following expression of the dielectric susceptibility tensor (11):

$$\epsilon_{jk} = \epsilon_0 \delta_{jk} + c_0 \epsilon_{jkl} S_l + c_2 N_{jk} \quad (12)$$

where $c_j = 2b_j/\omega^2$. In the language of optics, the scalar term proportional to c_0 corresponds to the isotropic polarizability of the atoms, while the vector term proportional to c_1 describes their optical activity around the axis defined by the atomic spin S . Finally, the tensor term proportional to c_2 gives birefringence effects, whose principal axis coincide with the ones of the nematicity ellipsoid defined as:

$$(N_{ij} + \frac{\delta_{ij}}{3} \rho) x_i x_j = 1 \quad (13)$$

The coefficients c_i depend on the internal structure of the excited state. Since the ground state has been assumed to have spin $F_g = 1$, absorbing a photon can excite the atoms to states of angular momentum $F_e = 0; 1; 2$. For each value of F_e , we derive a simple expression for the D tensor that depends only on a single parameter which quantifies the strength of the transition. The relative values of the c_i 's are completely determined by the angular momentum of the excited state. For notational simplicity we omit the angular brackets denoting expectation values of matter field operators.

For $F_e = 0$, the D tensor in cartesian components ($j; k = x; y; z$) has the form $D_{0jk} = D_0 \delta_{jk}$, so the dielectric susceptibility tensor is:

$$\epsilon_{jk} = \epsilon_0 \delta_{jk} + A_0 m_{jk} = \epsilon_0 \delta_{jk} + \frac{A_0}{3} \delta_{jk} + \frac{i}{2} \epsilon_{jkl} S_l + N_{jk} \quad (14)$$

i.e. $c_0^{(0)} = A_0/3$, $c_1^{(0)} = A_0/2$, and $c_2^{(0)} = A_0$ with $A_0 = 2\mathcal{D}_0^2/\hbar^2 \omega^2$ ($\mathcal{D}_0 = \langle 1_0 | \hat{D} | 0_0 \rangle$). This result has a simple interpretation: a photon polarized along the cartesian axis

j interacts only with the component of the matter field along the same axis.

For $F_e = 1$, the cartesian ($j, k, l = x, y, z$) components of the D tensor have the form $D_{jkl} = D_1 \delta_{jkl}$ and therefore one has:

$$\begin{aligned} jk &= jk + A_1 [jk - m_{kj}] \\ &= jk + A_1 \frac{2}{3} jk + \frac{i}{2} \delta_{jkl} S_1 - N_{jk} ; \quad (15) \end{aligned}$$

ie. $c_0^{(1)} = 2A_1=3$, $c_1^{(1)} = A_1=2$, and $c_2^{(1)} = A_1$ with $A_1 = 2j_1^2 j \sim 2! (1! 1_0)$. In physical terms, this means that light interacts only with the matter field polarized along direction orthogonal to the electric field polarization.

Finally, for $F_e = 2$, the dielectric susceptibility has the form :

$$\begin{aligned} jk &= A_2 \left[\frac{h_1}{2} jk + \frac{1}{2} m_{kj} - \frac{1}{3} m_{jk} \right] \\ &= A_2 \left[\frac{5}{9} jk - \frac{5i}{12} \delta_{jkl} S_1 + \frac{1}{6} N_{jk} \right] ; \quad (16) \end{aligned}$$

ie. $c_0^{(2)} = 5A_2=9$, $c_1^{(2)} = 5A_2=12$, and $c_2^{(2)} = A_2=6$.

If more than one excited state is involved in the optical process, the effective coupling U of the ground state atoms to the light is given by the sum of the contributions (3) of each single excited state, each of them being weighted by a factor $1/(\Gamma_i \Gamma)$, where Γ_i is the excitation energy and Γ the light frequency. Clearly, the result will be dominated by the states which are closest to resonance. By tuning to frequencies where the contributions from different excited states cancel, one can make at least one of the coefficients $c_{0,1,2}$ vanish.

Considerable simplification is found if the detuning is large compared to either the fine or hyperfine splitting. Consider the fundamental $nS \rightarrow nP$ transition of an alkali atom such as ^{23}Na or ^{87}Rb : the $S = 1=2$ electronic spin couples to the excited state's $L = 1$ electronic orbital angular momentum to produce two components of total electronic angular momentum $J = 1=2$ or $3=2$. The $L = 0$ ground state does not show any fine structure. Both ^{23}Na and ^{87}Rb have a nuclear spin of $I = 3=2$: coupling between the nuclear and electronic spins therefore result in the ground state splitting into two hyperfine components with $F = 2$ and $F = 1$ (in this paper we limit ourselves to $F = 1$). The $J = 1=2; 3=2$ components of the excited state respectively split into two hyperfine components of $F = 1; 2$, and four hyperfine components of $F = 0; 1; 2; 3$. For these alkali atoms, the fine structure separation is of the order of THz. Hyperfine structure, resulting from the much weaker coupling between the electron and the nucleus, is on the much smaller GHz energy scale.

If the detuning of the light is large with respect to the hyperfine splitting, the nucleus, whose direct coupling to

radiation is extremely weak, is not expected to play any role in the dynamics. In this regime, the frequency denominators in the U tensors (3) of the different hyperfine components are approximately equal. Consequently, U acts as the identity matrix in the space of nuclear states. It immediately follows that the dielectric function (11) only depends on the electronic part of the atomic density matrix, $m^{(e)} = \text{Tr}_n [n] = \sum_{m_I} \langle m_I | n | m_I \rangle$, where the index m_I runs over the $2I + 1$ possible nuclear spin states. As the total electronic angular momentum is $1=2$, the same symmetry arguments previously used to obtain the decomposition (12) now give the further constraint that $c_2 = b_2 = 0$, so that no birefringence effect nor any mechanical coupling of light to the nematic order parameter N can be present. The coefficients c_1 and c_0 will, however, generally be non-zero.

If the detuning of the light is also large with respect to the fine-structure splitting, then one can neglect the coupling between light and the electronic spin. The sum in (3) then traces out all of the spin degrees of freedom (both electronic and nuclear), leaving only the electronic orbital angular momentum. Consequently, in addition to $c_2 = b_2 = 0$, we have $c_1 = b_1 = 0$, and the atoms behave as a gas of spherically symmetric scatterers, with an isotropic dielectric susceptibility. In this regime, the mechanical coupling between light and the atoms does not depend on their initial state. This effect is currently exploited in optical traps in order to obtain a confining potential which traps all spin states in the same way [14].

The simple dependence of the dielectric tensor on the spin and nematic order parameters (12) is an useful starting point for optically imaging the order parameter of a spin 1 atomic sample. As a simple example, consider a thin, pancake-shaped, Bose-Einstein condensate which is rotating around the symmetry axis \hat{z} . Depending on the relative value of the s-wave scattering lengths $a_{0,2}$ in respectively the singlet and quintuplet channels, the ground state of the system in the rotating frame show completely different textures [5]. As two specific examples, gs.1a and 2a show the nematicity and spin and patterns for the antiferromagnetic $a_0 < a_2$ and the ferromagnetic case $a_2 < a_0$ under rotation. In the former case, the condensate shows defects such as π -dislocations in the nematic order parameter N , while the spin S vanishes outside of the cores of these defects. In the latter case, the condensate shows a spin pattern, while the nematic order parameter $N^2 = \sum_{ij} N_{ij}^2$ is everywhere vanishing.

We imagine that the imaging beam propagates along \hat{z} , ie. parallel to the rotation axis, and its polarization before interacting with the atoms is given by the two-component, generally complex polarization vector $p_{in} = (p_x; p_y)$. We assume the cloud is optically thin and that the length scale of the spin pattern is much larger than the optical wavelength used for the imaging, so that diffraction effects during the propagation through

the cloud can be neglected and the atomic density matrix ρ can be treated as locally uniform. Both of these assumptions are always valid if the cloud is allowed to expand ballistically before imaging. The polarization of the transmitted beam at the transverse position $\mathbf{x}_?$ after propagation through the cloud is then given by the following expression in terms of a column integral along the line of sight:

$$\rho_{out}(\mathbf{x}_?) = e^{i\mathbf{z} \cdot \mathbf{c}} \left[1 + \frac{i!}{c} \int_0^Z dz (n(\mathbf{x}_?; z) - 1) \right] \rho_{in} \quad (17)$$

The assumption that the cloud is optically thin implies that the magnitude of the term involving the integral is much smaller than unity. The matrix $n(\mathbf{x}_?; z)$, giving the local refractive index at the spatial position $(\mathbf{x}_?; z)$, is defined as the square root of the reduced dielectric tensor $\epsilon^{(xy)} = P_? P_?$, where $P_?$ is the projection operator orthogonal to the \hat{z} axis. As one can easily see from (12), $\epsilon^{(xy)}$ depends on the S_z component of the spin and on the $N_{xx}, N_{yy}, N_{xy}, N_{yx}$ components of the nematic order parameter only.

If the incident beam is circularly polarized σ , the density n and the spin component S_z both only give a phase shift. On the other hand, the nematicity can mix the two circular polarizations. We assume that the frequency of the imaging light is chosen so that the coupling c_2 to the nematicity N does not vanish. Then, if one illuminates the cloud with pure σ polarized light of amplitude c_+ , the σ component of the field after crossing the cloud has the amplitude:

$$c_+^{(0)} e^{i\mathbf{z} \cdot \mathbf{c}} \left[1 + \frac{i! c_2}{4c} \int_0^Z dz [N_{xx} - N_{yy} + i(N_{xy} + N_{yx})] \right] \quad (18)$$

In geometrical terms, a σ component is generated as soon as the (elliptical) cross-section of the nematicity ellipsoid (13) along the $z = 0$ plane is not circular. After blocking with a polarizer the original σ component, the intensity of the transmitted light $I = j^? j^?$ will be proportional to the square of the column integral of the reduced nematicity parameter

$$kN k^2 = (N_{xx} - N_{yy})^2 + \text{Re}[2N_{xy}]^2 \quad (19)$$

along the xy plane. In g.1b we have plotted the simulated intensity profile for a dislocation in a trapped rotating antiferromagnetic ($a_2 > a_0$) spinor condensate. In the $m_z = (1; 0; -1)$ basis, we have taken a condensate wavefunction of the form:

$$\psi(\mathbf{x}; y) = \frac{1}{\sqrt{2\pi}} \int_0^{2\pi} d\theta \exp\left[i\theta + i\frac{h}{2a^2}(\mathbf{x}^2 + y^2)\right] \quad (20)$$

with $u = 1/22$ and the harmonic oscillator length a of the order of μm [5]. The corresponding structure of the nematic order parameter is shown in g.1a. In this speci-

case, the magnitude of the nematicity $kN k$ is symmetric under rotations around the \hat{z} axis. The principal axes of N_{ij} rotate by π upon circling the disclination center.

More information on the geometrical structure of the nematic order parameter can be extracted by using phase-contrast techniques. Denoting with θ the angle between the \hat{x} axis and the minor axis of the nematicity ellipsoid, it follows from (18) that the phase of the generated σ component makes an angle 2θ with respect to the incident σ component. When this σ component is mixed with the incident σ component (with a mixing phase ϕ) in a typical phase-contrast scheme [15], the deviation of the detected intensity from its background value will be proportional to the quadrature $\text{Re}[e^{i\phi} - e^{i(\phi + 2\theta)}]$. As an example of such an images, we have plotted in g.1c a simulated image for the $\phi = 0$ case. The phase of the generated σ at points \mathbf{x} and \mathbf{x}' differ by ϕ as a result of the different orientation of the nematic order parameter. Changing the mixing phase rotates this image by ϕ .

In experiments on liquid crystals [12], one typically images using linearly polarized light. A crossed polarizer on the other side of the sample selects out the orthogonal component of the transmitted light. If the nematic order parameter is not parallel or perpendicular to the incident polarization plane, the polarization plane is rotated, and light will be transmitted through the crossed polarizer. The same approach can be used here, however, the optically active regions where $S_z \neq 0$ can also rotate the polarization plane, making it more difficult to analyze the images. One can isolate the contribution from the nematic order by working at a frequency at which the coupling of light to the spin vanishes, i.e. $c_1 = 0$. A simulated image is shown in g.1d for incident light polarized along x : the detected intensity is maximum along the \hat{y} axis where the nematic order parameter makes an angle $\theta = 45^\circ$ with \hat{x} .

We can isolate the contribution from the atomic spin S by working at a detuning which is large compared to the hyperfine structure of the excited state. In this case, $c_2 = 0$ and there is no mixing of the σ components. The difference between the phase shifts of the σ components results in the rotation of the polarization plane of a linearly polarized beam by an angle θ_{rot} , which depends on the column integral of S_z as,

$$\theta_{rot} = \frac{i! c_1}{2c} \int_0^Z dz S_z \quad (21)$$

The intensity of linearly polarized light passing through a crossed polarizer will be proportional to $\sin^2(\theta_{rot})$, which in the limit of an optically thin sample is just θ_{rot}^2 . One can thus get a direct measurement of the integrated magnitude of the \hat{z} component of the atomic spins. In g.1e, S_z is plotted for the π -disclination, and in g.1f, a simulated image is shown.

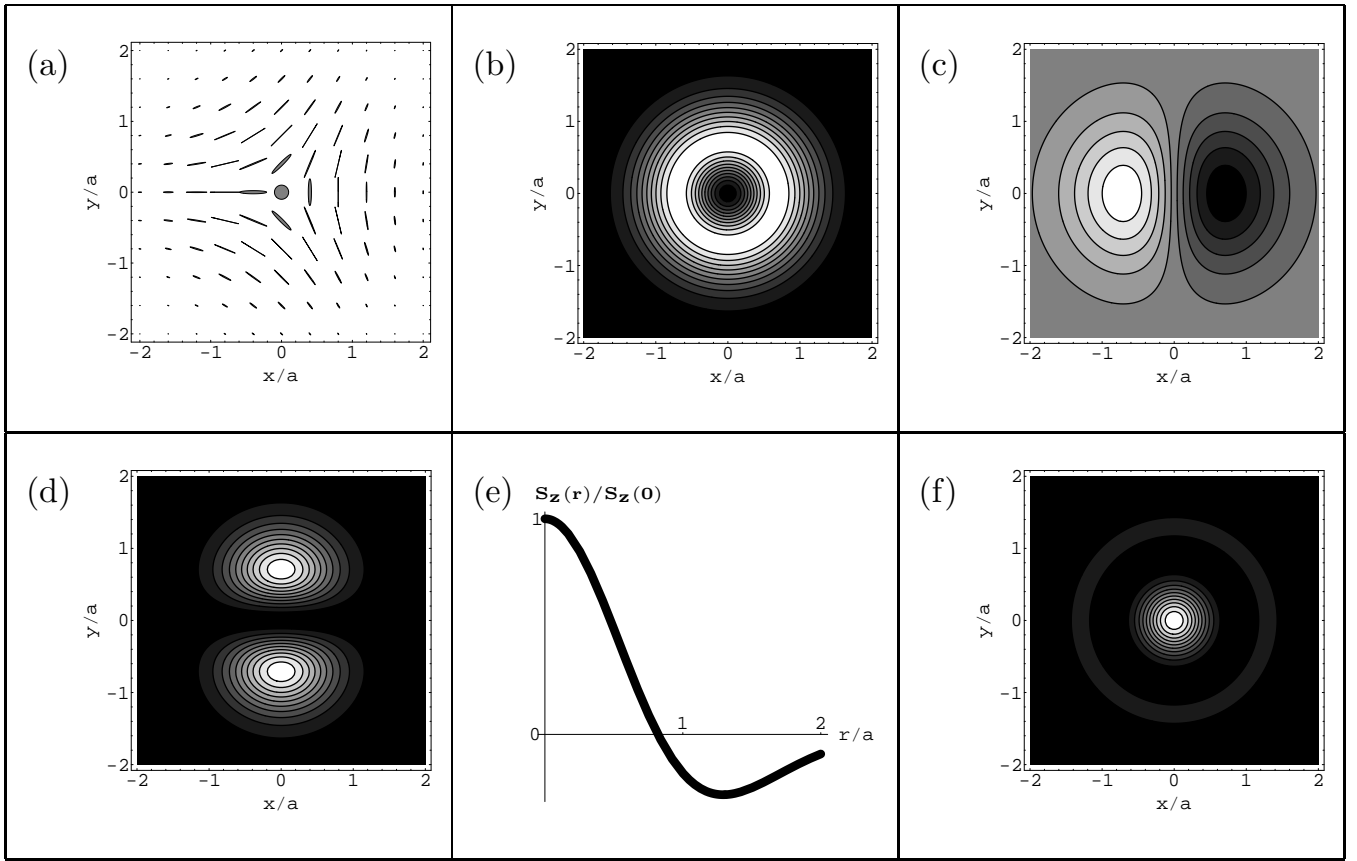


FIG. 1: Panel (a): Nematic order of a disclination in a rotating spinor BEC with antiferromagnetic interactions trapped in a harmonic trap of characteristic length a . Two dimensional projections of the nematicity ellipsoids (13) are shown on a regular grid. Away from the center the ellipsoids are degenerate and appear as rods. Panel (b,c): Images of the disclination using circularly polarized + probe light. The intensity of the generated component is shown in (b) and a phase-contrast image after mixing with the incident light (with phase = 0) is shown in (c). Panel (d): Image of the disclination using linearly polarized light and a crossed polarizer, when $c_1 = 0$. Panel (e): The \hat{z} component of the spin S_z , as a function of radial position. Panel (f): Image of the disclination using linearly polarized light and a crossed polarizer when the detuning is much greater than the hyperfine splitting so that $c_2 = 0$.

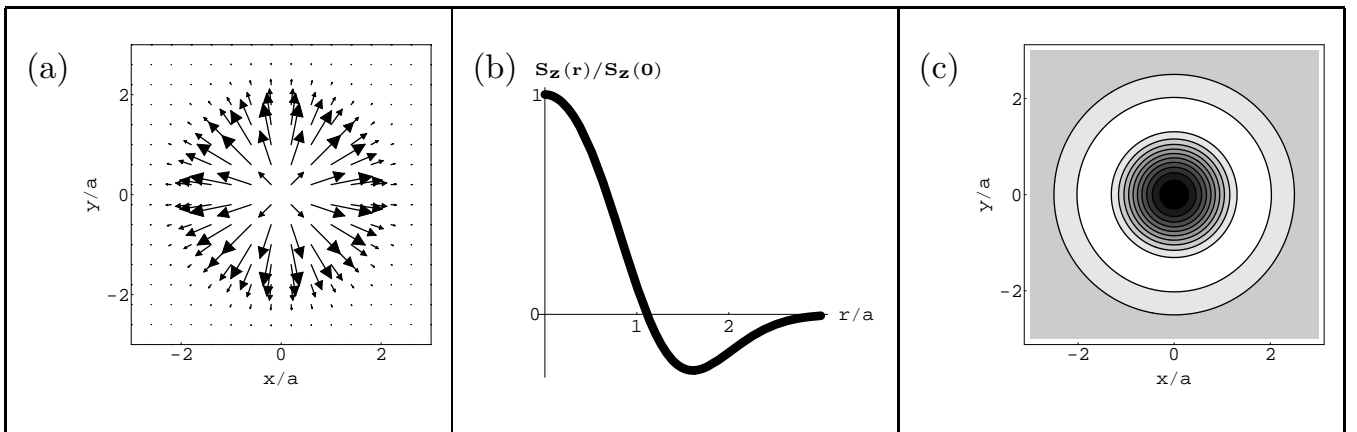


FIG. 2: Panel (a,b): geometrical structure of a skyrmion in a trapped rotating spinor BEC with ferromagnetic interactions. In (a), arrows represent the in-plane component of the spin, while (b) shows the radial dependence of the \hat{z} component. Panel (c): image of the skyrmion by detecting the phase difference between the transmitted components.

Since ϕ_{rot} corresponds to the phase shift between the components, one can also measure it via phase contrast techniques. In Fig. 2c we show a simulated phase contrast image of a texture in a ferromagnetic gas. This ^4He skyrmion has a wavefunction in the $m_z = (1; 0; 1)$ basis given by:

$$\psi(x; y) = \frac{1}{\sqrt{2}} \begin{pmatrix} 0 \\ v(x + iy)^2 \\ 1 \end{pmatrix} \exp\left(-\frac{h}{2a^2}(x^2 + y^2)\right) \quad (22)$$

with $u = 1.03$, $v = 0.81$, and is illustrated in 2a,b. In the external region, the spins point downwards, while they reverse direction as one approaches the center. Consequently, the image in Fig. 2c shows a low intensity region at the center, and a higher intensity region on a ring of radius $1.8a_{\text{ho}}$.

If the system shows a repeated pattern of vortices or -dislocations instead of a single one, the imaging may be better performed in the far-field plane. The amplitude of the Bragg-diffracted light in the direction $(k_x; k_y)$ is proportional to the Fourier transform of the emerging field after interaction with the cloud. As an example, we have plotted in Fig. 3b the Bragg diffraction pattern for the lattice of -disclinations shown in Fig. 3a; the incident light is $+$ polarized and diffracted light is observed. The periodicity of the lattice results in an evenly spaced series of isolated diffraction peaks whose strengths and geometrical arrangement give the detailed geometry of the lattice.

In summary, we have presented a novel technique for the in-situ imaging of spin textures in gaseous spin-1 atomic Bose-Einstein condensates. The technique is based on the dependence of the dielectric tensor on the local value of the density and of the spin and nematic order parameters. By considering a series of different spin textures, and detection geometries, we demonstrated how a range of physical quantities, such as the z component of the spin, and the magnitude and the orientation of the nematic order parameter can be imaged.

This polarized imaging technique could also be used to distinguish between states with and without spin order. For example, both nematic and spin singlet states have been predicted for antiferromagnetically interacting spin-1 atoms in an optical lattice [17].

We acknowledge hospitality at the Benaissance Center for Science and the Aspen Center for Physics where most of the present work has been done. I.C. acknowledges a Marie Curie grant from the EU under contract number HPMF-CT-2000-00901. Laboratoire Kastler Brossel is a Unité de Recherche de l'École Normale Supérieure et de l'Université Paris 6, associée au CNRS.

- [1] K. W. Madison, F. Chevy, W. Wohlleben, and J. Dalibard, Phys. Rev. Lett. 84, 806 (2000); J. R. Abo-Shaeer, C. Raman, J. M. Vogels, and W. Ketterle, Science 292, 476 (2001); P. C. Haljan, I. Coddington, P. Engels, and E. A. Comell, Phys. Rev. Lett. 87, 210403 (2001); E. Hodby, G. Hechenblaikner, S. A. Hopkins, O. M. Marago, and C. J. Foot, Phys. Rev. Lett. 88, 010405 (2002).
- [2] D. Vollhardt and P. Wolfle, The Superfluid Phases of Helium 3 (Taylor & Francis, London, 1990).
- [3] E. H. Aifer, B. B. Goldberg and D. A. Broido, Phys. Rev. Lett. 76, 680 (1996); S. E. Barrett, G. Dabbagh, L. N. Pfeiffer, K. W. West and R. Tycko, Phys. Rev. Lett. 74, 5112 (1995).
- [4] T. In-Lun Ho, Phys. Rev. Lett. 81, 742 (1998); T. Ohmichi and K. Machida, J. Phys. Soc. Jpn. 67, 1822 (1998); S.-K. Yip, Phys. Rev. Lett. 83, 4677 (1999); T. Isoshima, K. Machida, and T. Ohmichi, J. Soc. Jpn. 70, 1604 (2001); T. Mizushima, K. Machida and T. Kita, Phys. Rev. Lett. 89, 030401 (2002); Tomoya Isoshima, and Kazushige Machida, Phys. Rev. A 66, 023602 (2002); J.-P. Martikainen, A. Collin, and K.-A. Suominen, Phys. Rev. A 66, 053604 (2002); T. Mizushima, K. Machida, and T. Kita, Phys. Rev. A 66, 053610 (2002); T. Kita, T. Mizushima, and K. Machida, Phys. Rev. A 66, 061601 (2002); J. W. Reijnders, F. J. M. van Lankvelt, K. Schoutens, and N. Read, cond-mat/0306402.
- [5] E. J. Mueller, cond-mat/0309511.
- [6] M. R. Matthews, B. P. Anderson, P. C. Haljan, D. S. Hall, C. E. Wieman, and E. A. Comell, Phys. Rev. Lett. 83, 2498 (1999).
- [7] A. E. Leanhardt, Y. Shin, D. Kielpinski, D. E. Pritchard, and W. Ketterle, Phys. Rev. Lett. 90, 140403 (2003).
- [8] H. Schmalthann, M. Ehard, J. Kronjäger, M. Kottke, S. van Staa, J. J. Arlt, K. Bongs, and K. Sengstock, cond-mat/0308281; M.-S. Chang, C. D. Hamley, M. D. Barrett, J. A. Sauer, K. M. Fortier, W. Zhang, L. You, M. S. Chapman, cond-mat/0309164.
- [9] Unlike the other experiments, reference [6] was able to perform in-situ imaging of the spin texture by taking advantage of the fact that the different pseudo-spin components actually belonged to different hyperfine levels.
- [10] W. Gerlach and O. Stern, Zeitschrift Für Physik, 9, 349 (1922).
- [11] R. J. Epstein, I. Malajovich, R. K. Kawakami, Y. Chye, M. Hanson, P. M. Petrov, A. C. Gossard, and D. D. Awschalom, Phys. Rev. B 65, 121202(R) (2002); R. K. Kawakami, Y. Kato, M. Hanson, I. Malajovich, J. M. Stephens, E. Johnston-Halperin, G. Salis, A. C. Gossard, D. D. Awschalom, Science 294, 131 (2001).
- [12] S. Chandrasekhar, Liquid Crystals, Second Edition, Cambridge University Press, Cambridge (1992).
- [13] The cartesian components $(\hat{x}; \hat{y}; \hat{z})$ are related to the more familiar spherical components $(\hat{1}; \hat{0}; \hat{-1})$ [where the subscript refers to the spin projection in the \hat{z} direction] by $\hat{x} = (\hat{1} - \hat{-1})/\sqrt{2}$; $\hat{y} = i(\hat{1} + \hat{-1})/\sqrt{2}$; $\hat{z} = \hat{0}$.
- [14] C. S. Adams and E. Riis, Prog. Quant. Electr. 21, 1 (1997).
- [15] M. Born and E. Wolf, Principles of optics, Cambridge University Press, Cambridge (1959).

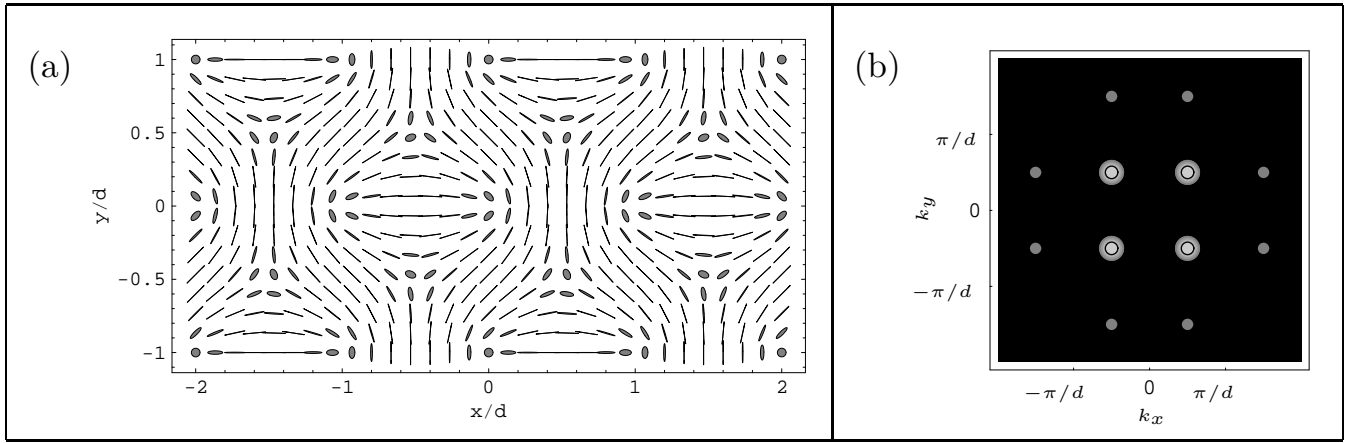


FIG. 3: Panel (a): Nematic order in array of disclinations. The closest distance between disclinations whose cores have the same spin polarization is d . Panel (b): Diffraction pattern seen in σ light when σ light is incident on this array of disclinations.

- [16] A. M. Dudarev, R. B. Diener, I. Carusotto, and Q. Niu, (2002).
in preparation (2003).
- [17] E. Demler and F. Zhou, Phys. Rev. Lett. 88 163001,